



Assessment of Wall Deflections and Ground Settlements for Braced Excavations Subjected to Groundwater Drawdown: Numerical Simulations and Design Charts

Runhong Zhang, Ph.D., Smart City Research Institute, Chongqing University, Liyang, Jiangsu, China; College of Aerospace Engineering, Chongqing University, Chongqing, China; email: zhangrh@cqu.edu.cn

Wengang Zhang, Professor, School of Civil Engineering, Chongqing University, Chongqing, China; email: cheungwg@126.com

Anthony Goh Teck Chee, Associate Professor, School of Civil and Environmental Engineering, Nanyang Technological University, Singapore; email: ctcgoh@ntu.edu.sg

ABSTRACT: *Due to the dense population and limited space in urban areas, the development of underground space is desirable, highlighting the importance of deep excavation. Deep excavations in soft clay deposits may cause excessive ground movements and thus result in potential damage to adjacent buildings and supporting utilities. This paper describes the general project and site conditions of four Mass Rapid Transit (MRT) stations of Downtown Line Stage 2 (DTL2): Cashew, Hillview, Bukit Panjang, and Beauty World. Then the paper summarizes the field performance of braced excavations in Bukit Timah Granite (BTG) residual soils, based on the instrumented data from the four sites. Extensive finite element analyses were carried out to develop a series of base case design charts for assessing the wall deflections and ground settlements for braced excavations in BTG residual soils. The modification factors are also proposed, indicating the influences of groundwater drawdown, system stiffness, excavation width, excavation depth, and rock head level above the final elevation level on wall deflections and ground settlements, respectively. A comparison between the measured results from the sites and the predictions based on base cases validated the rationality and feasibility of the proposed modification factors, as well as the presented design charts.*

KEYWORDS: BTG residual soil, braced excavation, wall deflection, ground settlement, groundwater drawdown, design charts.

SITE LOCATION: [Geo-Database](#)

INTRODUCTION

Many underground infrastructure developments are very actively being carried out in Singapore. Land Transport Authority (LTA) Singapore sets the civil design criteria for road and rail transit systems, stating that both temporary and permanent works shall be designed to ensure that ground movements are kept to an absolute minimum. It's also worth noting that the use of proven construction techniques and good workmanship are essential in minimizing ground loss and water table drawdown (LTA 2019). The construction of these underground works close to existing buildings could potentially result in excessive ground movements, which could lead to adjacent buildings' damage. Consequently, this could lead to costly litigation and time-consuming remedial works as well as the delay on the completion of major projects. Therefore, an understanding of the general excavation system behavior from braced excavation activities is essential.

There are many empirical and semi-empirical methods for relating the excavation-induced maximum wall deflections to the basic design parameters, including the excavation depth and width, the thickness of soft soils and the system stiffness or the relative stiffness ratios (Mana and Clough 1981; Wong and Broms 1989; Clough and O'Rourke 1990; Hashash and Whittle 1996; Addenbrooke et al. 2000; Kung et al. 2007; Zhang et al. 2015; Goh et al. 2017). However, limited approaches can be referred to when it comes to estimating the excavation-induced ground surface settlements, with the exception of the

Submitted: 17 January 2020; Published: 10 August 2021

Reference: Zhang R., Zhang W., Goh A.T.C. (2021). Assessment of Wall Deflections and Ground Settlements for Braced Excavations Subjected to Groundwater Drawdown: Numerical Simulations and Design Charts. International Journal of Geotechnical Engineering Case Histories, Volume 6, Issue 2, pp. 67-80, doi: 10.4417/IJGCH-06-02-04



previous charts proposed over the last century (Peck 1969; Clough and O'Rourke 1990; Ou et al. 1993; Hsieh and Ou 1998), and their modifications (Hsieh and Ou 1998; Kung et al. 2007; Cham and Goh 2011; Goh et al. 2020). The reasons might lie in that: firstly, the ground surface settlement response is more complicated and is generally monitored by settlement markers at different distances from behind the wall, while for the wall deflection response, the wall inclinometer instrumentation is much easier; secondly, the maximum ground surface settlement is generally within 0.5-1.0 times the maximum wall deflections for braced excavations only when the ground surface settlement is solely caused by the wall deflection without considering the groundwater drawdown (Mana and Clough 1981; O'Rourke 1981; Goh et al. 2017).

Groundwater drawdowns can be caused by potential wall leakage, flow from beneath the wall embedded in the residual soils with more percentiles of silts or sandy silts, flow from perched water along with the wall interface, or poor panel connections due to less satisfactory quality. For cases with considerable groundwater drawdowns behind the excavation, consolidation settlements are induced due to the increased effective stresses as a result of the groundwater drawdown, leading to a much more significant measured total ground surface settlement. Some studies have focused on underground excavations in permeable strata and analyzed the leakage and seepage problems (Zheng et al. 2014; Shen et al. 2017; Tan and Lu 2017; Tang et al. 2017; Zeng et al. 2018). However, case histories with significant groundwater drawdown outside the excavation, an incident which leads to an excessive ground settlement, were rarely reported (Wen and Lin 2002; Laefer et al. 2003, 2006; Zhang et al. 2018a, 2018b).

An overview of the general project and site conditions for the four stations of Downtown Line Stage 2 (DTL2) is provided in this study, followed by a summary of the measured field performances for braced excavations in BTG residual soils. Extensive finite element analyses were carried out to develop a series of base case design charts for assessing the wall deflections and ground settlements. This study also presented modification factors accounting for the influences of groundwater drawdown, system stiffness, excavation width, excavation depth, and rock head level above the final elevation level GIII (e.g., grade III-moderately weathered rock mass) above Final Elevation Level (FEL) on excavation responses. Procedures and design charts developed for assessing the wall deflections and the ground settlements for braced excavations in BTG residual soils were in agreement with the field instrument records.

PROJECT DESCRIPTION AND FIELD INSTRUMENTATIONS

Project Overview

As the fifth MRT line in Singapore, Downtown Line (DTL) is a major MRT line directly linking the downtown area with the northern and eastern parts of the city. It is being implemented in three stages; Stage 2 (DTL2), with its 16.6 km twin tunnel and 12 underground stations, was completed in December 2015. Figure 1 shows the location of the reported project, comprised mainly of four sites with four cut-and-cover braced excavations for the construction: 1) the Bukit Panjang station for Site C912; 2) the Cashew and Hillview stations for Site C913; 3) the Beauty World station for C916; and 4) Site C915 which is mainly comprised of the tunnels. Figure 1 also briefly summarizes the ground conditions. Generally, the ground consists of Fill, Kallang Formation (F), Bukit Timah granite residual soils (Grade VI: GVI), completely weathered materials (Grade V: GV), highly weathered materials (Grade IV: GIV), and moderately weathered to fresh rock (Grade III to I: GIII to GI). The groundwater table ranges from 0.4 m to 4.4 m below the ground surface level. More studies related to this project are referred to Zhang and Goh (2016), Zhang et al. (2018a, b), and Zhang et al. (2019).

Figure 2 shows the typical cross-sectional view and the soil profiles based on existing boreholes. This figure also presents the typical geologic units, the generalized site stratigraphy, and the relative position between each strut level and geologic unit. It should be noted that the four sites are located in the ground of the predominant igneous rocks and weathered soils of the Bukit Timah Granite, as well as the marginal soft clays and loose sands of the Kallang Formation. The adjacent building types are mostly residential blocks and shop houses.

Table 1 summarizes the range and average of Standard Penetration Test SPT-N values for both F and GVI for each station. Table 2 summarizes the ranges of soft soil thickness (F and GVI), the groundwater drawdown d_w , and the depth of the rockhead GIII (or GIV) for each station. A summary of the mechanical and physical properties of Singapore Bukit Timah Granite residual soils and rocks can be referred to Veeresh and Goh (2017), Ip et al. (2019), Zhang et al. (2019), and Goh et al. (2020).

Figure 3 plots the variation of soil compositions with depth for BTG residual soil as well as the liquid limit (LL), the plastic limit (PL), and the plasticity index (PI) changes with depth based on borehole DT2439 of the Cashew site.

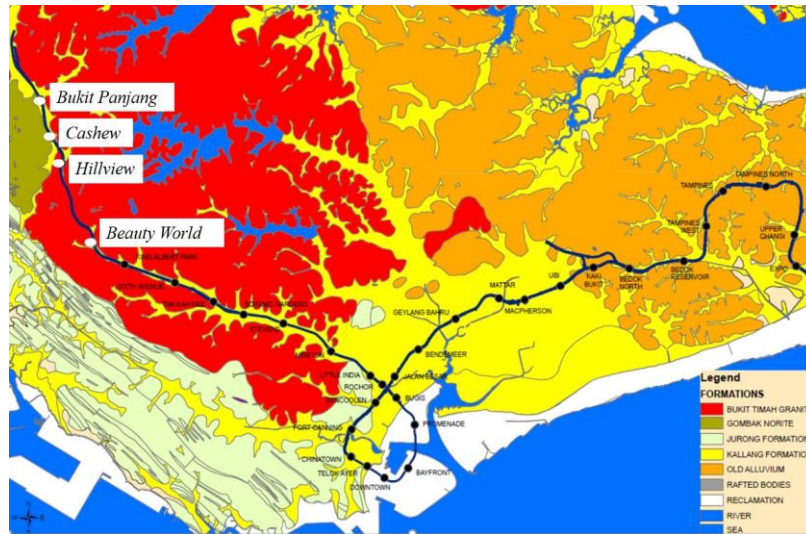


Figure 1. Four sites of DTL2: Cashew, Hillview, Beauty World, and Bukit Panjang (Figure from LTA website, www.lta.gov.sg).

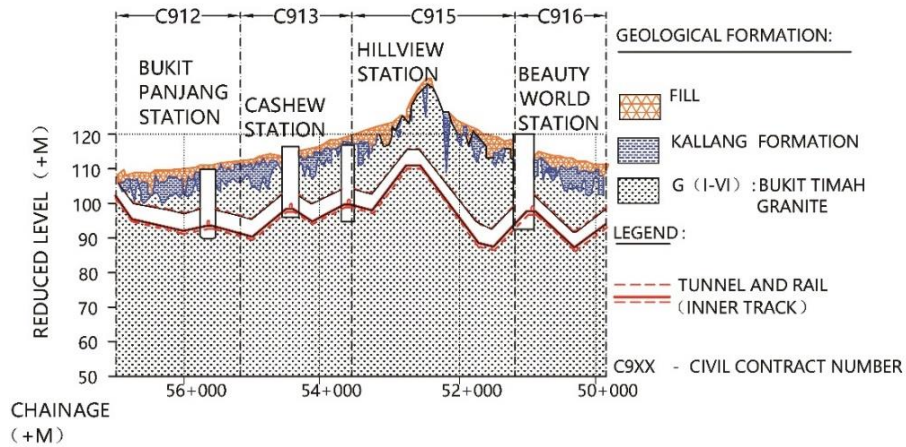


Figure 2. Typical geological soil profiles and cross-sectional view (after Zhang et al. 2019).

Table 1. SPT-N values for Kallang Formation and GVI.

Stations	Kallang Formation		GVI	
	Ranges	Ave.	Ranges	Ave.
Cashew	2~16	7	2~52	17
Hillview	0~18	8	4~52	18
Bukit Panjang	2~17	9	2~42	16
Beauty World	1~14	6	2~44	15

Table 2. Summary of ranges of soft soil thickness, d_w , and the depth of the rock head.

Station	d_w (m)	Thickness of F	Thickness of GVI	Depth of GIII
Cashew	12.4 ~ 15.9	1.3 ~ 9.0	3.0 ~ 19.0	17.6 ~ 35.5
Hillview	12.8 ~ 23.4	3.0 ~ 8.5	3.0 ~ 30	15.0 ~ 35.5
Bukit Panjang	1.8 ~ 5.8	5.0 ~ 9.0	2.6 ~ 9.0	13.5 ~ 27.7
Beauty World	2.0 ~ 7.2	7.0 ~ 9.0	2.9 ~ 8.5	9.0 ~ 29.8

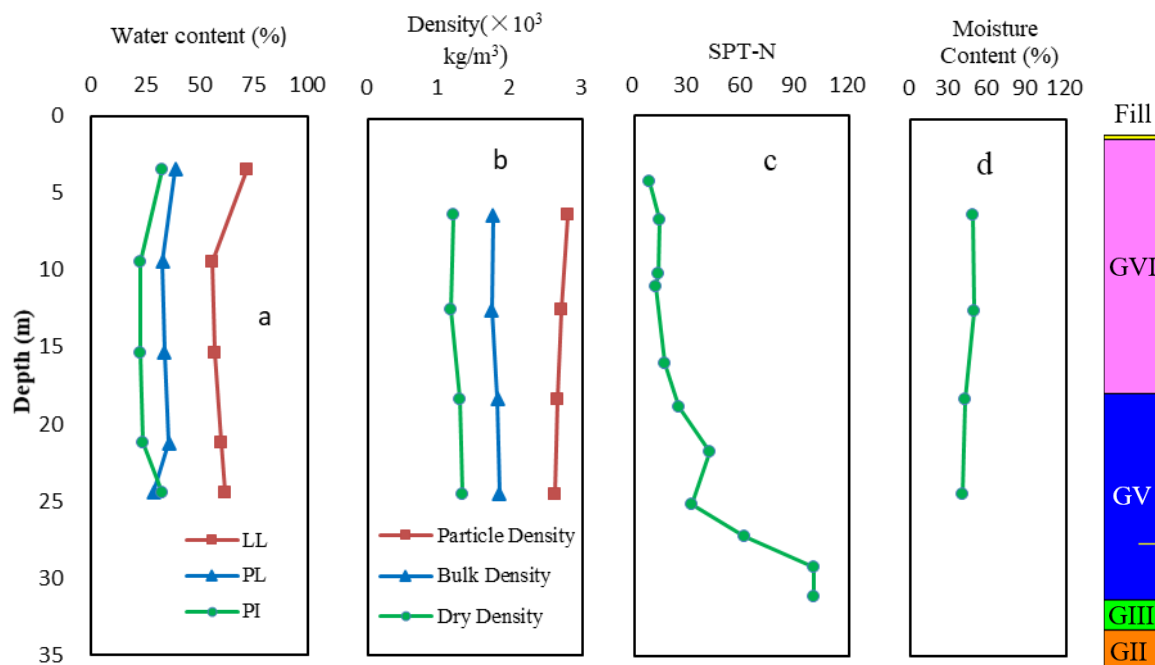


Figure 3. Variation of index properties with depth for BTG residual soil (based on borehole DT2439).

Supporting Systems

Table 3 summarizes the wall type for each station, including the secant bored pile (SBP) and diaphragm wall (D-wall), the number of strut levels, preloading conditions, and the depth of the final elevation level (FEL).

Table 3. Excavation support system description for each station.

Station	Depth of FEL	Wall system	Strut levels	Strut and preloading condition
Bukit Panjang	22 m	SBP (1.2 m)	5	Both reinforced concrete and steel struts used with spacing at 9.0 m c/c for horizontal strut with splays; bracket welded to runner beam. Struts preloaded.
Cashew	20 m	D-wall (1.0 m)	4	Strut: HY 700, waler beam: HY700 with bracket HY400; the struts are preloaded to 100% of design load from 100 to 350 kN/m (1st level: 100 kN/m, 2nd level: 300 kN/m, 3rd & 4th levels: 350 kN/m).
Hillview	24 m	D-wall (1.0 m & 1.2 m)	6	HY 700 struts. Double waler beam HY650 is used. Both runner beam and knee strut are HR 350. Struts preloaded to 100% of design load (1st level: 100 kN/m, 2nd level: 200 kN/m, 3rd level: 400 kN/m, 4th, 5th & 6th levels: 500 kN/m).
Beauty World	20 m	SBP (1.2 m)	4	Struts spacing at 8.5 m c/c with pre-loading (S1: 150 kN, S2: 270 kN, S3: 350 kN, S4: 400 kN). The strut sizes are: S1 – 2-UB 400×300×94.3 kg/m; S2 – 2-UB 500×300×128 kg/m; S3 & S4 – 2-UB 610×324×155 kg/m.

Field Instrumentations

Figures 4 summarizes the instrumentation schemes and measurement types for the Cashew station. The collected monitoring data are as follows:

- (a) Diaphragm wall and secant bored pile wall deflections (using in-wall inclinometers);



- (b) Pore water pressures (using vibrating wire piezometers);
- (c) Ground settlements (using settlement markers); and
- (d) Strut loadings (using strain gauges and load cells).

For which data from the inclinometers and piezometers were obtained daily during excavation. Notations of the symbols are as follows: I: inclinometer; GWV: vibrating wire piezometer; LG: ground settlement marker; SG: strain gauge; LC: load cell.

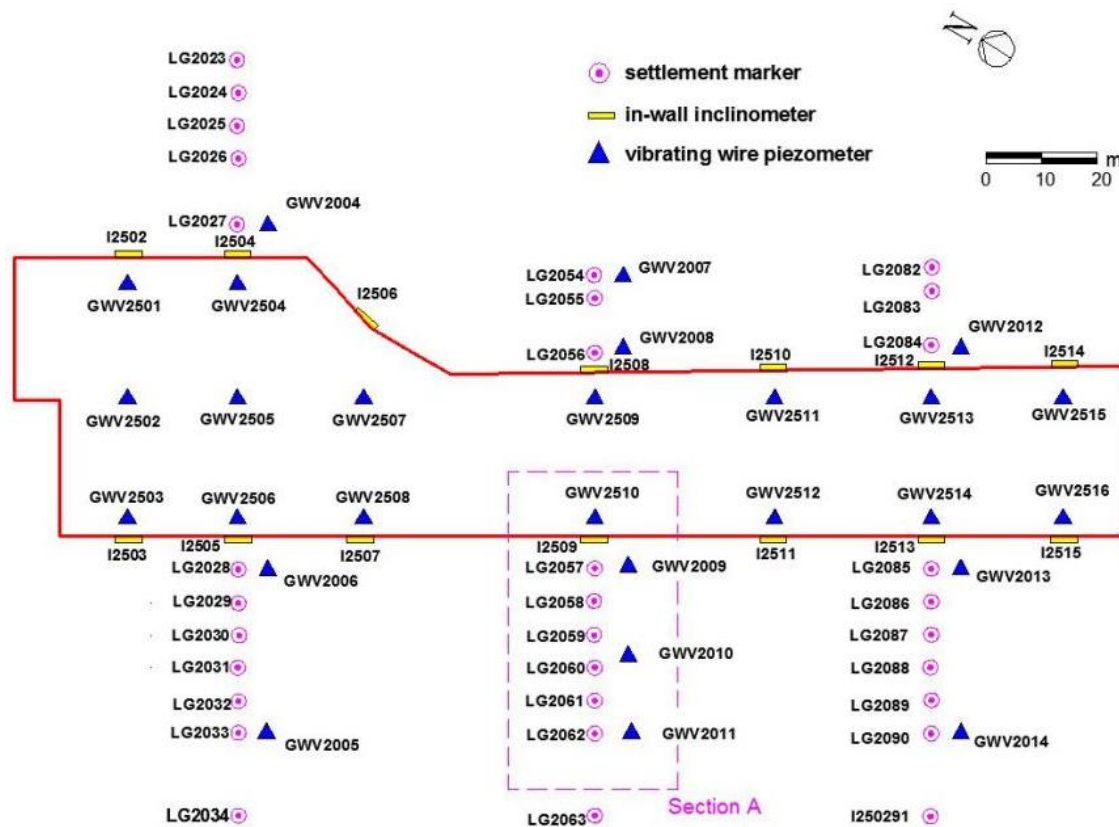


Figure 4. Instrumentation schemes and types for the Cashew station. (after Zhang et al. 2018a)

NUMERICAL CALIBRATION

According to Zhang et al. (2018a), a two-dimensional plane-strain finite element (FE) model was developed using the software PLAXIS 2D (Brinkgreve 2017), based on Section A of Figure 4. The soils were simulated by 15-node triangular elements with a hardening soil (HS) elastoplastic constitutive model, adopting the Duncan-Chang hyperbolic model and Mohr-Coulomb failure criterion, which is proper in the simulation of excavations in view of its hardening behaviors. The input parameters are shown in Table 4. Figure 5 shows the schematic cross-section of the excavation system. The diaphragm walls were modeled by linear elastic plate elements, with $EA=2.8 \times 10^7$ kN/m and $EI=1.8 \times 10^6$ kN m²/m. Struts were considered as liner elastic fixed-end anchors, ignoring the potential bending behavior. Considering the extra load from surrounding infrastructures, a surcharge of 20 kPa was applied on the ground surface within a zone of 20 m away from the excavation. The initial groundwater level was 2 m below the ground surface. The simulation details, the numerical schemes, and the excavation procedures can be referred to in Zhang et al. (2018a). Figure 6 indicates that the magnitudes of the computed lateral displacement are generally in agreement with the measured results, and the underestimation of the maximum ground settlement is less than 2%. The numerical simulation results are reasonably consistent with the measured data.

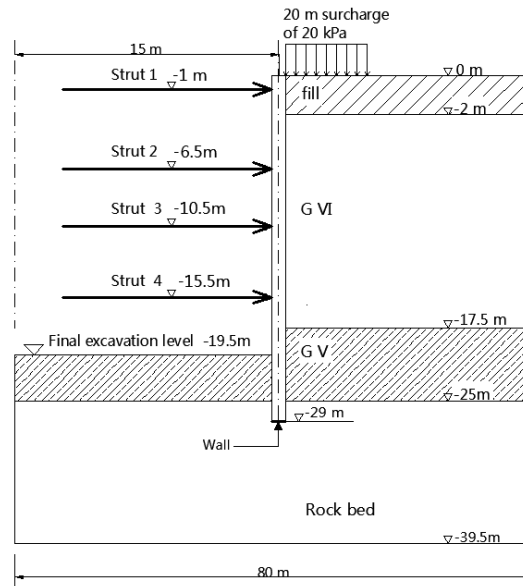


Figure 5. Numerical model (after Zhang et al. 2018a).

Table 4. Material parameters used for numerical simulation (after Zhang et al. 2018a).

Material	γ_{unsat} (kN/m ³)	γ_{sat} (kN/m ³)	E_{50}^{ref} (MPa)	$E_{\text{oed}}^{\text{ref}}$ (MPa)	$E_{\text{ur}}^{\text{ref}}$ (MPa)	m	c' (kPa)	ϕ' (°)
Fill	16	18.5	7	6	19.5	0.6	0.1	30
GVI	16	18.5	8	6.5	24	0.6	0.1	30
GV	17	19	16	14	48	0.6	0.1	33
Bedrock	24	24	200	200	600	0	300	45

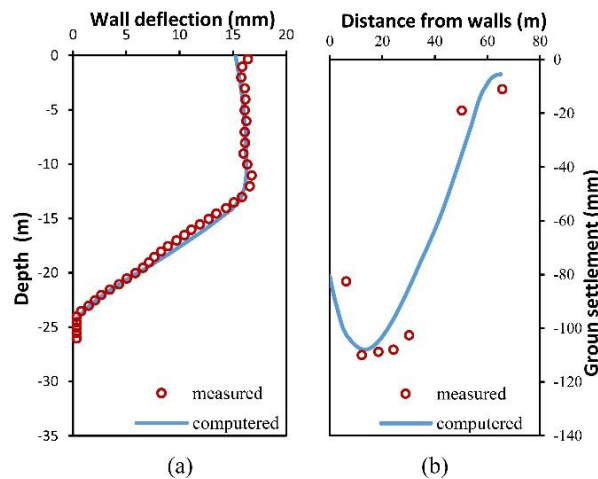


Figure 6. Comparisons of measured and computed excavation responses (after Zhang et al. 2018a).

PARAMETRIC ANALYSIS AND MODIFICATION FACTORS

The aforementioned calibrated numerical model was adopted for the parametric analysis.

Range of Parameters

Using the Hardening Soil (HS) model with relative stiffness ratio $E_0/c_u = 250$ and the derived soil correlations, a parametric study was carried out to assess the influence of the thickness of the GVI layer, the groundwater drawdown d_w , and the SPT-N value of GVI on the wall deflection and ground settlement. Table 5 lists the range of the design parameters considered.



Table 5. Range of parameters.

Parameters	Values
GVI thickness (m)	6~20
Groundwater drawdown d_w (m)	0~16
SPT-N of GVI	2~25
Excavation depth (m)	17~31
Excavation width (m)	20~40
System stiffness	446~1452
Thickness of GIII above FEL(m)	-8~8

Influences on Ground Surface Settlements

Figure 7 shows the influence of the thickness of the GVI layer and the groundwater drawdown d_w on the maximum ground surface settlement (δ_{vm}) for different SPT-N values of GVI. In Figure 7a, where N equals 2, the calculated factor of safety against the basal heave is less than 1.0 when GVI is thicker than 10 m, so the δ_{vm} is unavailable. The δ_{vm} increases with the increase in d_w . The general trend is that the maximum ground settlement increases as the GVI thickness increases. Furthermore, the δ_{vm} decreases significantly as the SPT-N value increases.

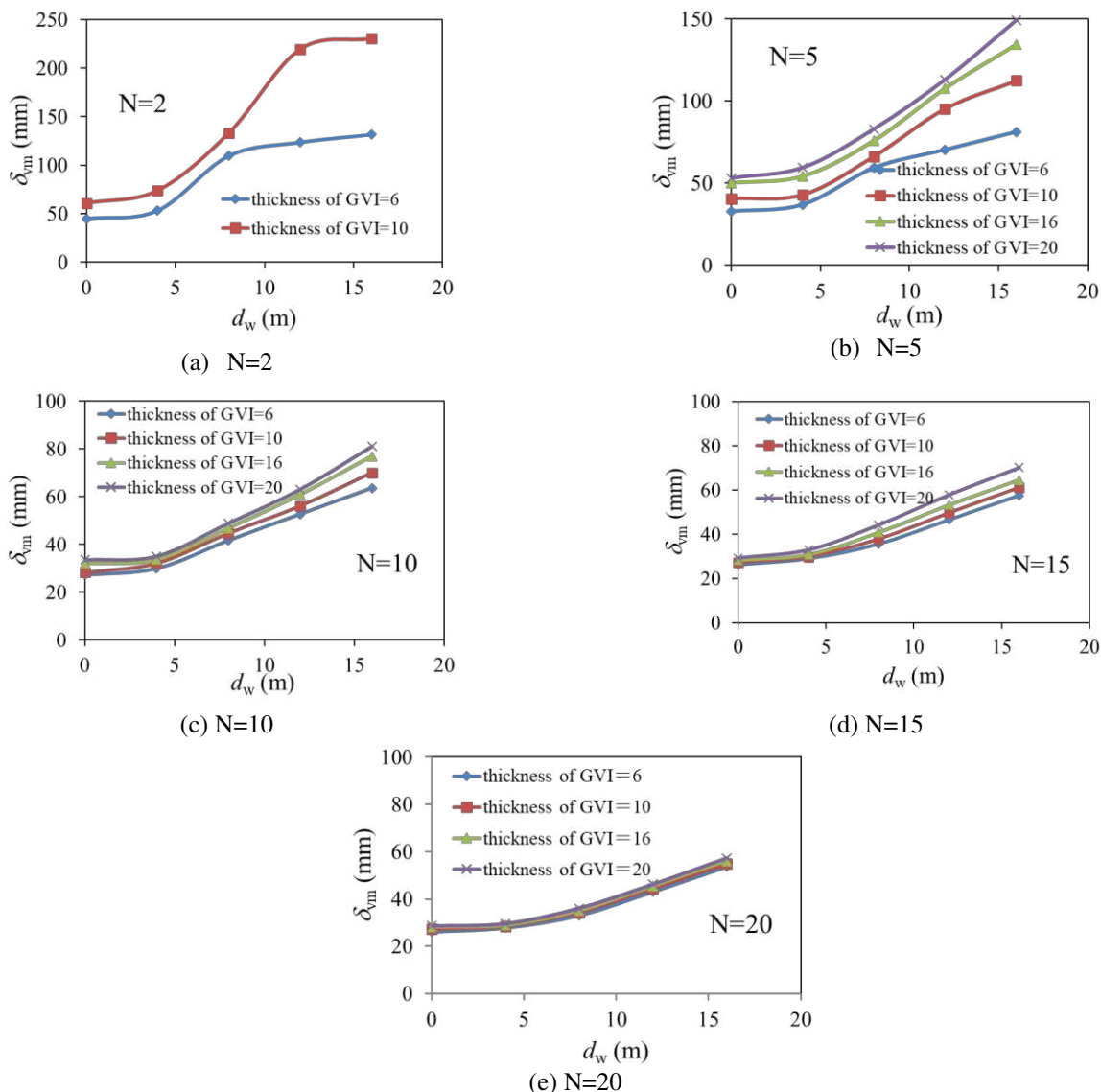


Figure 7. Effect of thickness of the GVI layer and the groundwater drawdown d_w on the δ_{vm} for different N values.



Influences on Wall Deflections

Figure 8 shows the influence of GVI thickness and the groundwater drawdown d_w on the wall deflection for different SPT-N values of GVI. The maximum wall deflection (δ_{hm}) decreases as the groundwater drawdown increases. However, the decrease of wall deflection is marginal, especially when the drawdown d_w is greater than 4 m. The general trend is that the δ_{hm} increases with an increase of GVI thickness and decreases as the SPT-N increases.

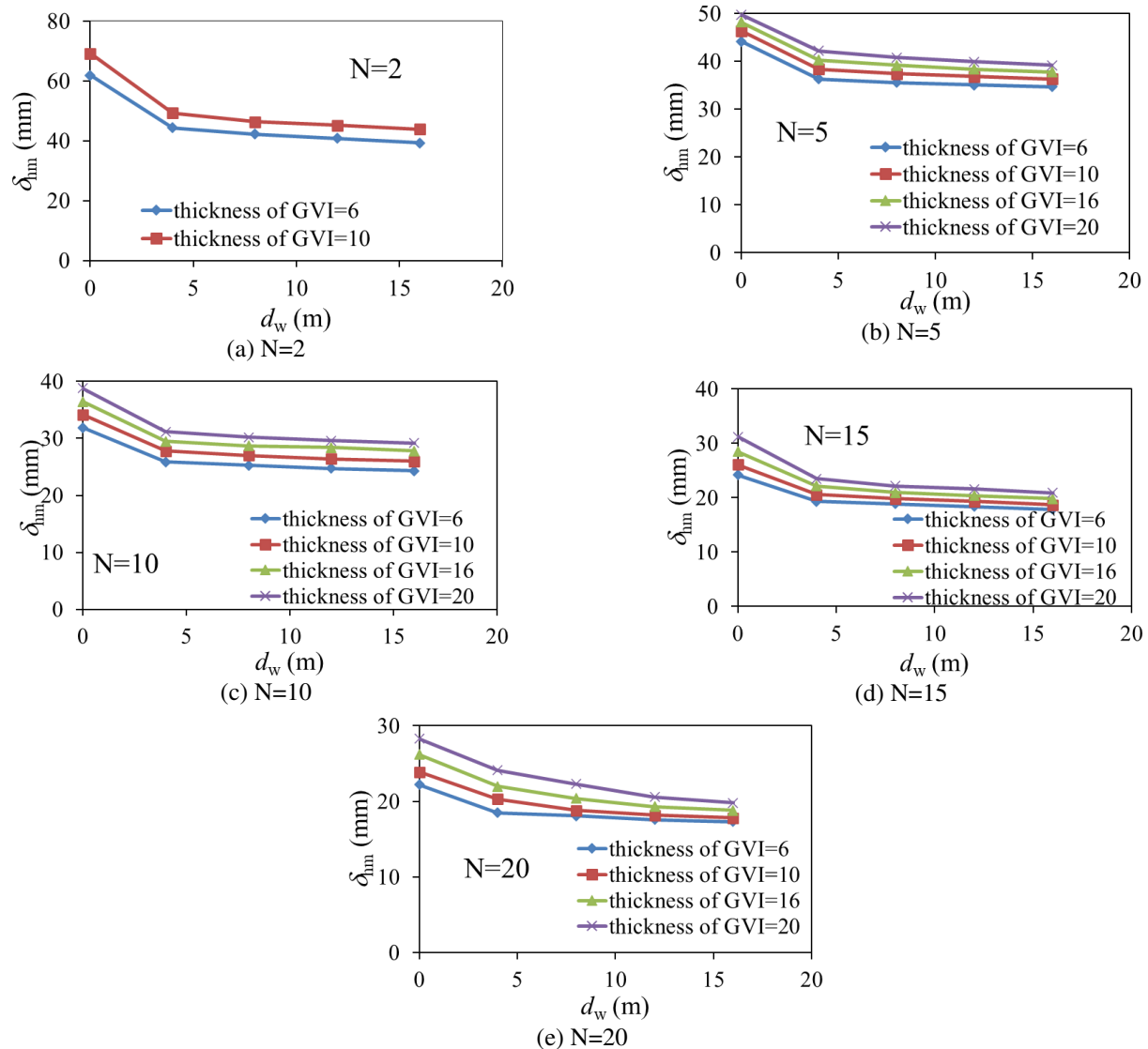


Figure 8. Effect of thickness of the GVI layer and d_w on wall deflection for different N values.

Modification Factors and the Proposed Design Charts

The proposed charts for assessing wall deflection and ground settlement comprise a series of base design charts and modification factors. Design charts are functions of SPT-N and thickness of the GVI layer. Modification factors are accountable for the influences of groundwater drawdown, system stiffness, excavation width, excavation depth, and rock head level above the final elevation level (GIII above FEL) on excavation responses. This study adopted the system stiffness S proposed by Clough and O'Rourke (1990), which can be expressed as:

$$S = (EI)_{wall} / (\gamma_w h_{avg}^4) \quad (1)$$



where $(EI)_{wall}$ is the wall stiffness, γ_w is the unit weight of water, and h_{avg} is the average vertical strut spacing.

The base design charts are developed based on parameter combinations of system stiffness $S=462$, excavation width $B= 30$ m, excavation depth $H_e= 20$ m, GIII above FEL= -4 m (4 m below FEL), and $d_w= 0$ m. Figure 9 shows the base design charts for δ_{hm}/H_e and δ_{vm}/H_e , respectively.

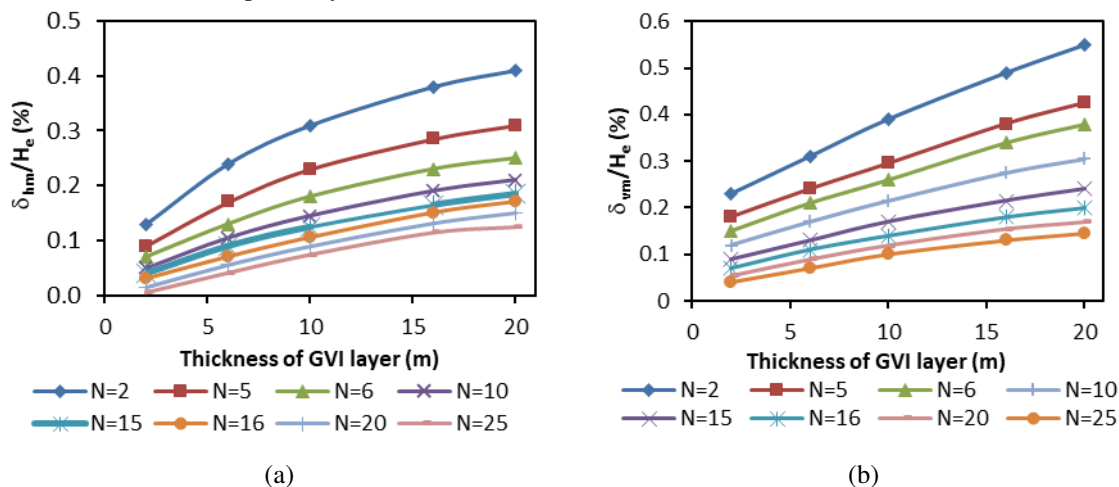


Figure 9. Base design charts for: (a) δ_{hm}/H_e , (b) δ_{vm}/H_e .

The modification factors include:

- μ_S : modification factors of system stiffness;
- μ_B : modification factors of excavation width;
- μ_{H_e} : modification factors of excavation depth;
- $\mu_{GIII \text{ above FEL}}$: modification factors of the thickness of GIII above FEL;
- μ_{d_w} : modification factors of groundwater drawdown.

For δ_{vm} , $\mu_S=1.0$ since the influence of system stiffness is marginal. Figure 10 plots μ_S for δ_{hm} . The μ_S values for different S are listed in Table 6.

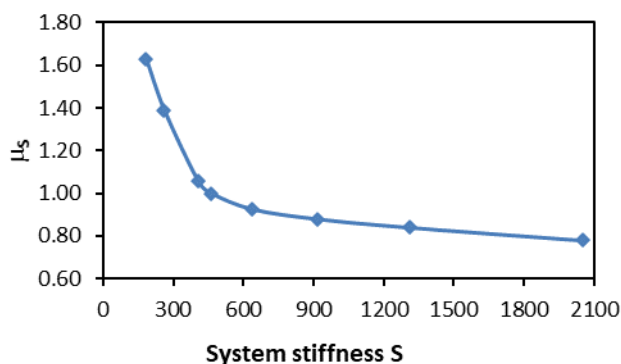


Figure 10. μ_S chart for δ_{hm} .

Table 6. Suggested μ_S values for different S for δ_{hm} .

S	446	462	588	1020	1452
μ_S	1.03	1.00	0.93	0.86	0.83

μ_B , $\mu_{GIII \text{ above FEL}}$, and μ_{d_w} for δ_{hm} and δ_{vm} are plotted in Figures 11, 12, and 13, respectively. μ_{H_e} for δ_{hm} is listed in Table 7. The influence of excavation depth on δ_{vm} is marginal. Thus, $\mu_{H_e}=1.0$ for δ_{vm} .

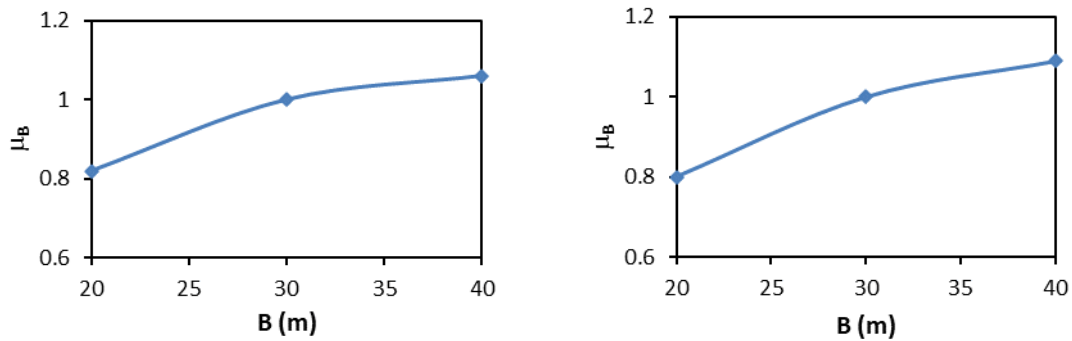


Figure 11. μ_B chart for (a) δ_{hm} , and (b) δ_{vm} .

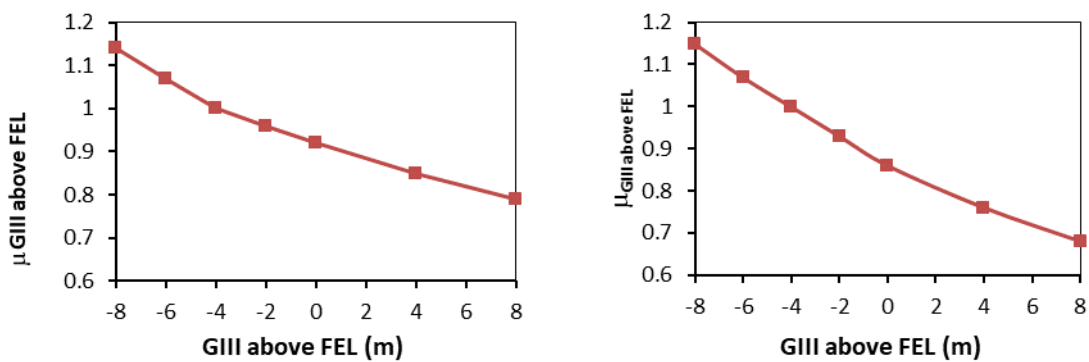


Figure 12. $\mu_{GIII \text{ above FEL}}$ chart for (a) δ_{hm} , and (b) δ_{vm} .

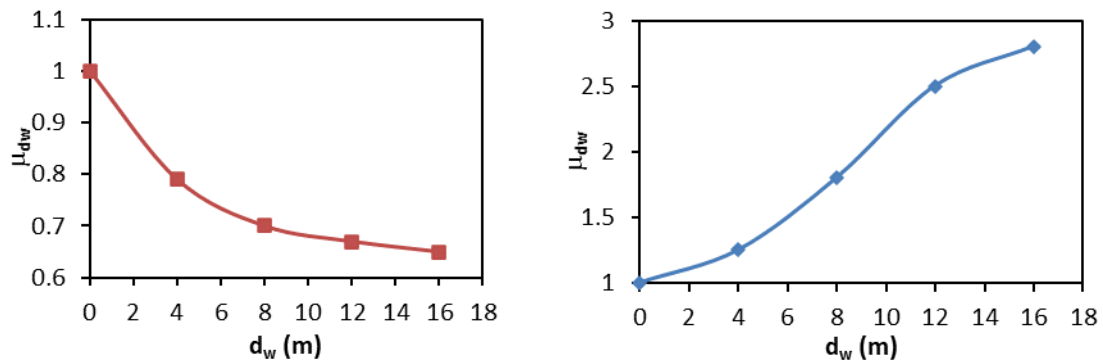


Figure 13. μ_{dw} chart for (a) δ_{hm} , and (b) δ_{vm} .

Table 7. Suggested μ_{He} values.

H_c (m)	17	20	21	25	31
μ_{He}	0.97	1.00	1.06	1.65	1.95

The advantage of the proposed charts in Figures 10-13, as well as Tables 6 and 7, is that no iteration is required for computing the wall deflection and ground settlement, which would be demonstrated in the section below. However, the further application of the proposed design charts is limited by the particular characteristics of the construction sites, including both the significant groundwater drawdown and the existence of the residual soils. Therefore, the use of the



proposed charts in similar braced excavation projects developed in residual granitic soils in Singapore is promising, while the extended applications should be more cautious.

VALIDATIONS FROM FIELD INSTRUMENTATIONS OF FOUR SITES

An Example Calculation on the Use of Modification Factors

This section presents an example calculation to show how to use the base case design charts as well as the modification factors to derive the lower and upper bound maximum wall deflection and ground surface settlement. Take the hypothetical case of GIII 2 m above FEL, $B = 20$ m, $H_e = 21$ m, $d_w = 12$ m, SPT $N = 10$, $T = 15$ m, $S = 650$, for example.

1. Since $N = 10$ and $T = 15$ m, from Figure 9, the $(\delta_{nm}/H_e)_b = 0.180$ and $(\delta_{vm}/H_e)_b = 0.285$;
2. Modification factor μ_S : $S = 650$, from Figure 10, the μ_S value for δ_{nm}/H_e is 0.91 while μ_S value for δ_{vm}/H_e is 1.0;
3. Modification factor μ_B : $B = 20$ m, from Figure 11, the μ_B value for δ_{nm}/H_e is 0.82 while μ_B value for δ_{vm}/H_e is 0.80; Modification factor $\mu_{GIII \text{ above FEL}}$: GIII is 2 m above FEL, from Figure 12, the $\mu_{GIII \text{ above FEL}}$ value for δ_{nm}/H_e is 0.89, while $\mu_{GIII \text{ above FEL}}$ for δ_{vm}/H_e is 0.80;
4. Modification factor μ_{d_w} : $d_w = 12$ m, from Figure 13, the μ_{d_w} value for δ_{nm}/H_e is 0.67, while μ_{d_w} for δ_{vm}/H_e is 2.51;
5. Modification factor μ_{H_e} : $H_e = 21$ m, from Table 7, the μ_{H_e} value for δ_{nm}/H_e is 1.06, while μ_{H_e} for δ_{vm}/H_e is 1.0; and
6. the actual $(\delta_{nm}/H_e)_a$ and $(\delta_{vm}/H_e)_a$ is derived from the following equation:

$$(\delta_{nm}/H_e)_a = (\delta_{nm}/H_e)_b \times \mu_S \times \mu_B \times \mu_{GIII \text{ above FEL}} \times \mu_{d_w} \times \mu_{H_e} \quad (2)$$

$$(\delta_{vm}/H_e)_a = (\delta_{vm}/H_e)_b \times \mu_S \times \mu_B \times \mu_{GIII \text{ above FEL}} \times \mu_{d_w} \times \mu_{H_e} \quad (3)$$

Thus, $(\delta_{nm}/H_e)_a = 0.180\% \times 0.91 \times 0.82 \times 0.89 \times 0.67 \times 1.06 = 0.085\%$ and $(\delta_{vm}/H_e)_a = 0.285\% \times 1.0 \times 0.80 \times 0.80 \times 2.51 \times 1.0 = 0.458\%$.

Validation with Field Measurements

A comparison plot between the measured results and the predicted results based on the proposed base design charts, together with the modification factors, indicates that they are in agreement with each other, as shown in Figures 14 and 15. The R^2 for the training and testing model are 0.9862 and 0.9817, respectively. Therefore, the proposed procedures, comprising of the base design charts and the modification factors, work well for the assessment of wall deflections and ground settlements for the braced excavations subjected to the drawdown of groundwater in BTG residual soils.

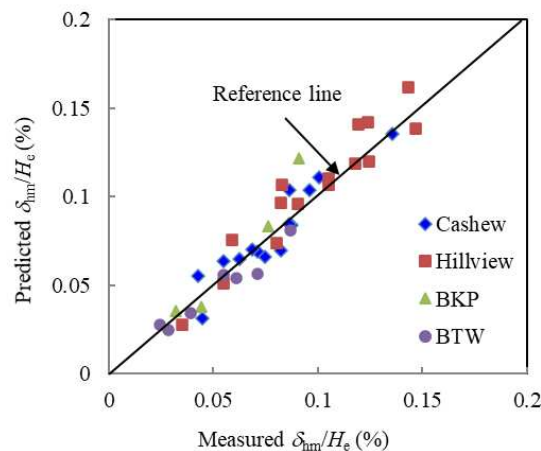


Figure 14. Predicted δ_{nm}/H_e vs. measured results.

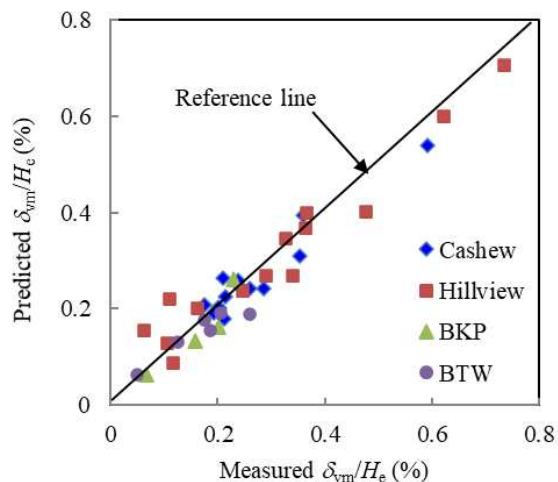


Figure 15. Predicted δ_{vm}/H_e vs. measured results.

DISCUSSION

In a braced excavation, the wall deflection and ground settlement may be significantly affected by the ground water drawdown, especially in areas of residual deposit soils, such as in Singapore, Taiwan, and Shanghai. Most of the existing predictive methods of the wall deflection and ground settlement were obtained based on field measurements and local experiences. In this study, the general trend is that: with the increases of d_w , δ_{vm} increases and δ_{hm} decreases, and the decrease of δ_{hm} is marginal when d_w is greater than 4 m. Due to the limitation of the data used for the design chart, it is more feasible for cases that the excavation depth is between 17 m and 31 m while the excavation width ranges from 20 m to 40 m, etc., as the ranges listed in Table 5.

Several cases reported by Goh et al. (2020) are used to calculate the δ_{vm} via the proposed design chart, and are compared to the predicted δ_{vm} derived from the artificial neuron network (ANN) by Goh et al. (2020). The case information is listed in Table 8. Table 9 shows the comparison between the ground settlement predicted by the proposed design chart δ_{vm-DC} and the δ_{vm-ANN} provided by Goh et al. (2020).

Table 8. Cases reported by Goh et al.(2020).

Case No.	S	B	H	d_G	d_w	$SPT N_{60}$
1	261	30	19.5	-6	14.9	16.2
2	261	30	19.5	-0.5	15.7	16
3	1090	30	20	0.2	4.4	8

Table 9. Comparison between the δ_{vm-DC} and δ_{vm-ANN} from Goh et al.(2020).

Case No.	$(\delta_{vm}/H_e)_b$	μ_s	μ_{GIII}	μ_{dw}	μ_{He}	μ_B	Measured δ_{vm-M}	δ_{vm-ANN}	$\delta_{vm-ANN}/\delta_{vm-M}$	$(\delta_{vm}/H_e)_a$	δ_{vm-DC}	$\delta_{vm-DC}/\delta_{vm-M}$
1	0.17	1	1.07	2.6	0.98	1	70.8	71	1.0	0.46	90.3	1.27
2	0.16	1	0.93	2.8	0.98	1	72.2	61	0.84	0.41	79.6	1.10
3	0.23	1	0.91	1.3	1.06	1	33	45	1.36	0.29	57.7	1.74

As shown in Table 9, the $\delta_{vm-DC}/\delta_{vm-M}$ is 1.27, 1.10, and 1.74 for Cases 1, 2 and 3 respectively, which are greater than those of $\delta_{vm-ANN}/\delta_{vm-M}$. The proposed design chart is prone to be conservative compared to the ANN method which was adopted by Goh et al. (2020). Despite that the accuracy of the proposed design chart is inferior to the ANN method, it's more user-friendly and capable of considering key influential factors, while the black-box ANN model is difficult to interpret, as indicated in the appendix of Goh et al. (2020).



Hopefully the proposed semi-empirical model based on the DTL excavation database may be used for design guidance and as a preliminary check for wall deflections and ground settlements for braced excavations subjected to drawdown of groundwater in BTG residual soils. However, the design engineers should be cautious about the use of the proposed design chart considering its limitations.

SUMMARY AND CONCLUSIONS

This study described the general project and site conditions for four DTL2 stations, followed by a summary of the field performances and instrumentations. Extensive finite element analyses were carried out to develop a series of base case design charts for assessing the wall deflections and ground settlements for braced excavations in BTG residual soils. Modification factors accounting for groundwater drawdown, system stiffness, excavation width, excavation depth, GIII above FEL, etc., were presented. The developed design charts with modification factors were found to be in agreement with the field instrumented records from the four stations. The design charts and the proposed modification factors may be used for design guidance for similar braced excavation projects developed in residual granitic soils in Singapore.

ACKNOWLEDGMENTS

This paper is part of the LTIF project titled "Braced Excavation-Induced Ground Movements", funded by the Land Transport Authority (LTA), Singapore. The authors would like to acknowledge the financial support provided by LTA. Special thanks to Dr. Goh Kok Hun and Mr. Otard Chew for their useful and insightful suggestions during the monthly meetings. The corresponding author is also grateful to the support of the National Natural Science Foundation of China (No. 52078086), the Program of Distinguished Young Scholars, Natural Science Foundation of Chongqing, China (cstc2020jcyj-jq0087).

REFERENCES

- Addenbrooke, T.I, Potts, D.M. and Dabee, B. (2000). "Displacement flexibility number for multiple retaining wall design". *Journal of Geotechnical and Geoenvironmental Engineering*, 126(8), 718–726.
- Brinkgreve, R.B.J., Kumarswamy, S. and Swolfs, W.M. (2017). *PLAXIS 2D 2017 user's manual*, PLAXIS bv, Netherlands.
- Clough, G.W. and O'Rourke, T.D, (1990). "Construction induced movements of in-situ walls. Design and Performance of Earth Retaining Structure". *Geotechnical Special Publication ASCE*, New York, 25, 439-470.
- Cham, W. M. and Goh, K. H. (2011), "Prediction of ground settlement due to adjacent deep excavation works." *Underground Singapore*, 94-103.
- Faheem, H., Cai, F., Ugai, K. and Hagiwara, T. (2003). "Two-dimensional base stability of excavations in soft soils using FEM." *Computers and Geotechnics*, 30(2), 141-163.
- Goh, A.T.C, Zhang, F., Zhang, W., Zhang, Y., and Liu, H. (2017). "A simple estimation model for 3D braced excavation wall deflection." *Computers and Geotechnics*, 83, 106-113.
- Goh, A.T.C, Zhang, R.H., Wang, W., Wang, L., Liu, H., and Zhang, W.G. (2020). "Numerical study of the effects of groundwater drawdown on ground settlement for excavation in residual soils." *Acta Geotechnica*, 15, 1259–1272.
- Hashash, Y.M.A, and Whittle, A.J. (1996). "Ground movement prediction for deep excavations in soft clay". *Journal of Geotechnical Engineering*, 122 (6), 474-486.
- Hsieh, P.G, and Ou, C.Y, (1998) "Shape of ground surface settlement profiles caused by excavation". *Canadian Geotechnical Journal*, 35(6), 1004-1017.
- Ip, C.Y.S., Rahardjo, H., Satyanaga, A. (2019). "Spatial variations of air-entry value for residual soils in Singapore". *Catena*, 174, 259-268.
- LTA Engineering Group. (2019). *Civil Design Criteria for Road and Rail Transit Systems. E.GD/09/106/A2 (Controlled document)*.
- Peck, R. B. (1969). "Deep excavation and tunneling in soft ground." *Proc. 7th Int. Conf on Soil Mechanics and Foundation Engineering*, 225-290.
- Klotz, U., Vermeer, P.A., Klotz, C., and Moller, S. (2006). "A 3D finite element simulation of a shield tunnel in weathered Singapore Bukit Timah Granite." *Tunnelling and Underground Space Technology*, 21(3-4), 272.
- Kung, G.T.C, Hsiao, E.C.L, and Juang, C.H. (2007) "Evaluation of a simplified small-strain soil model for analysis of excavation-induced movements". *Canadian Geotechnical Journal*, 44, 726-736.
- Laefer, D.F., Frazier, J. and Evans, A., (2003). "Dewatering induced settlement of a historic landmark." *Proc. International Geotechnical Conference Dedicated to the Tercentenary of Saint Petersburg*, ASV Publishers, St. Petersburg, Russia.



-
- Laefer, D.F., Evans, A., and Frazier, J. (2006). Forensic investigation methodology for structures experiencing settlement, *APT Bulletin*, 37(2-3), 23-31.
- Mana, A.I. and Clough, G.W. (1981). "Prediction of movements for braced cuts in clay." *Journal of Geotechnical Engineering*, 107(6), 759–777.
- Ou, C.Y., Hsieh, P.G. and Chiou, D.C. (1993) "Characteristics of ground surface settlement during excavation." *Canadian Geotechnical Journal*, 30(5), 758-767.
- Osborne, N.H., Yang, A., Macphie, D., Ra, S.H. and Soh, K.M. (2011) "Understanding the engineering behavior of Bukit Timah Granite during deep excavation and the benefits of early design review." *Underground Singapore*, 177–188.
- O'Rourke TD, (1981) "Ground movements caused by braced excavations." *Journal of Geotechnical Engineering Division ASCE*, 107(9), 1159-1178.
- Shen, S., Wu, Y., and Misra, A. (2017) "Calculation of head difference at two sides of a cut-off barrier during excavation dewatering." *Computers and Geotechnics*, 91, 192-202.
- Tan, Y., and Lu, Y. (2017) "Forensic diagnosis of a leaking accident during excavation." *Journal of Performance of Constructed Facilities*, 31(5).
- Tang, X., Gan, P., Liu, W., and Zhao, Y. (2017) "Surface settlements induced by tunneling in permeable strata: a case history of Shenzhen Metro." *Journal of Zhejiang University - SCIENCE A (Applied Physics and Engineering)*, 18(10), 757-75.
- Teng, F., Arboleda-Monsalve, L.G. and Finno, R. J. (2018). "Numerical Simulation of Recent Stress-History Effects on Excavation Responses in Soft Clays." *Journal of Geotechnical and Geoenvironmental Engineering*, 144(8).
- Veeresh, C., and Goh, K.H., (2017). "Bukit Timah Granite Formation Engineering Properties and Construction Challenges." *Geotechnical Engineering*, 48, 86-91.
- Wen, D., and Lin, K. (2002). "The effect of deep excavation on pore water pressure changes in the Old Alluvium and under-drainage of marine clay in Singapore" In Kastner, Emeriault, Dias, Guilloux (Eds.), *Geotechnical aspects of underground construction in soft ground*, Lyon, 447-452.
- Wong, K.S, and Broms, B.B. (1989) "Lateral wall deflections of braced excavation in clay." *Journal of Geotechnical Engineering*, 115 (6), 853–870.
- Zeng, C., Xue, X., Zheng, G., Xue, T., and Mei, G. (2018) "Responses of retaining wall and surrounding ground to pre-excavation dewatering in an alternated multi-aquifer aquitard system." *Journal of Hydrology*, 559-609.
- Zheng, G., Zeng, C., Diao, Y., and Xue, X. (2014). "Test and numerical research on wall deflections induced by pre-excavation dewatering." *Computers and Geotechnics*, 62, 244-256.
- Zhang, W., and Goh, A.T.C. (2015), "A simple prediction model for wall deflection caused by braced excavation in clay." *Computers and Geotechnics*, 63, 67-72.
- Zhang, W., and Goh, A.T.C. (2016). "General behavior of braced excavation in Bukit Timah Granite residual soils: a case study." *International Journal of Geoenvironmental Case Histories*, 3(3), 190-202.
- Zhang, W., Wang, W., Zhou, D., Zhang, R., Goh, A.T.C., and Hou, Z. (2018a) "Influence of groundwater drawdown on excavation responses - A case history in Bukit Timah granitic residual soils". *Journal of Rock Mechanics and Geotechnical Engineering*.
- Zhang, W., Goh, A.T.C, Goh, K.H., Chew, O.Y.S, Zhou, D., and Zhang, R. (2018b). "Performance of braced excavation in residual soil with groundwater drawdown." *Underground Space*, 3, 150–165.
- Zhang, W., Zhang, R., Han, L., and Goh, A.T.C. (2019). "Engineering properties of Bukit Timah Granitic residual soils in Singapore DTL2 braced excavations". *Underground Space*, 4(2), 98-108.



INTERNATIONAL JOURNAL OF
**GEOENGINEERING
CASE HISTORIES**

*The Journal's Open Access Mission is
generously supported by the following Organizations:*



Access the content of the *ISSMGE International Journal of Geoengineering Case Histories* at:
www.geocasehistoriesjournal.org